Food Research International 188 (2024) 114466

Contents lists available at ScienceDirect

Food Research International

journal homepage: www.elsevier.com/locate/foodres

Impact of pilot-scale microfluidization on soybean protein structure in powder and solution

Andreea Diana Kerezsi [a,b,*], Nicolas Jacquet [a], Oana Lelia Pop [b,c], Ines Othmeni [a,e], Antoine Figula [a], Frédéric Francis [d], Gaoussou Karamoko [e], Romdhane Karoui [e], Christophe Blecker [a]

[a] Gembloux Agro-Bio Tech, Department of Food Science and Formulation, University of Liège, 5030 Gembloux, Belgium
[b] Department of Food Science, University of Agricultural Sciences and Veterinary Medicine, Cluj-Napoca 400372, Romania
[c] Molecular Nutrition and Proteomics Laboratory, Institute of Life Sciences, University of Agricultural Sciences and Veterinary Medicine, Cluj-Napoca 400372, Romania
[d] Functional and Evolutionary Entomology, Gembloux Agro-Bio Tech, University of Liège, Gembloux 5030, Belgium
[e] Univ. Artois, Univ. Lille, Univ. Littoral Côte d'Opale, Univ. Picardie Jules Verne, Univ. de Liège, INRAE, Junia, UMR-T 1158, BioEcoAgro, F-62300 Lens, France

ARTICLE INFO

Keywords:
Shearing process
Protein modification
Structural changes

ABSTRACT

The effect of microfluidization treatment on the primary, secondary, and tertiary structure of soybean protein isolate (SPI) was investigated. The samples were treated with and without controlling the temperature and circulated in the system 1, 3, and 5 times at high pressure (137 MPa). Then, the treated samples were freeze-dried and reconstituted in water to check the impact of the microfluidization on two different states: powder and solution. Regarding the primary structure, the SDS-PAGE analysis under reducing conditions showed that the protein bands remained unchanged when exposed to microfluidization treatment. When the temperature was controlled for the samples in their powder state, a significant decrease in the quantities of β-sheet and random coil and a slight reduction in α-helix content was noticed. The observed decrease in β-sheet and the increase in β-turns in treated samples indicated that microfluidization may lead to protein unfolding, opening the hydrophobic regions. Additionally, a lower amount of α-helix suggests a higher protein flexibility. After reconstitution in water, a significant difference was observed only in α-helix, β-sheet and β-turn. Related to the tertiary structure, microfluidization increases the surface hydrophobicity. Among all the conditions tested, the samples where the temperature is controlled seem the most suitable.

1. Introduction

In recent years, researchers and consumers have shifted their attention more to plant-based proteins (Islam et al., 2023; Rodrigues et al., 2012), driven by their multiple health benefits and extensive utility within the food industry (Sui et al., 2021), economy and sustainability concerns (Aschemann-Witzel et al., 2021; Santo et al., 2020; De Boer & Aiking, 2011).

Among plant-based proteins, soybean (*Glycine* max) is well recognized for oil extraction and represents more than 50 % of oil production (Rodrigues et al., 2012). Besides this, the by-products obtained are valorized. They are also very important for human health (reduction of cholesterol and cardiovascular disease, improvement of bone health) due to the amino acid profile and high quality of proteins (Qin et al., 2022).

Progress in the food industry has led to the development of a range of soybean products such as flour, defatted meal, concentrates, isolates, and texturized products (Jideani, 2011). As a result of multiple varieties,

Abbreviations: 1PN, 3PN, and 5PN, The microfluidized samples where the temperature was not controlled, where 1, 3, and 5 represent the number of passes; 1PW, 3PW, and 5PW, The microfluidized samples where the temperature was controlled; ANS, 1-anilinonaphthalene-8-sulfonic acid; ATR, Attenuated total reflectance; C, Control – a non-microfluidized sample; DHPM, Dynamic high-pressure microfluidization; FI, Fluorescence intensity; F_{max}, Maximum fluorescence; FTIR, Fourier Transform Infrared Spectroscopy; If/g × μM, Intensity fluorescence/gram × microMolar – measurement unit for PSH; MF, Microfluidization/Microfluidized; MIR, Mid-infrared spectroscopy; PSH, Protein surface hydrophobicity; SDS-PAGE, Sodium dodecyl sulfate–polyacrylamide gel electrophoresis; SPI, Soy protein isolate; λ_{max}, Maximum emission wavelength.

* Corresponding author.
E-mail addresses: adkerezsi@uliege.be, andreeadianakerezsi@gmail.com (A. Diana Kerezsi).

https://doi.org/10.1016/j.foodres.2024.114466
Received 8 December 2023; Received in revised form 27 March 2024; Accepted 1 May 2024
Available online 3 May 2024

soybean product consumption has increased in the past years. Soybean protein isolate is one of the most discussed soybean ingredients obtained by isoelectric precipitation (Lee et al., 2016; Jideani, 2011) and contains 90 % or more proteins (Codex Alimentarius, 2022).

In order to enhance the functional properties given by soybean proteins, covering solubility, foaming ability, emulsification, gel formation, and more, different physical treatments have been investigated for their advantages, such as improving the organoleptic properties (texture, flavor, color, aroma) and maintaining the levels of antioxidants and phenolic compounds in the final product (Dong et al., 2020).

To date, high-pressure homogenization, high hydrostatic pressure, microfluidization, ultrasonication, and similar techniques play a pivotal role. These processes are applied to improve functional properties and induce structural changes in proteins. Recently, Hu et al., 2023 reported an increase in emulsification activity (5.81–29.6 %) and emulsion stability (5.31–25.9 %) at pressure from 20 to 100 MPa for the high-pressure homogenization, with a heat treatment was applied beforehand. This treatment increases the surface hydrophobicity of the SPI and reduces the random coils and β-sheets, forming soluble aggregates and improving the emulsifying properties. Additionally, Martínez et al., 2011 highlighted that subjecting the SPI-hydroxypropylmethylcellulose mixtures to dynamic high-pressure treatment (up to 300 MPa) will enhance foaming properties. It is observed that these processes can be applied directly to protein ingredients, such as SPI, to modify their functionality.

Further, their functionality can be used in food formulations to obtain a final product. Moreover, besides improving functional properties, some of these treatments were recognized to reduce soybean allergens. Recently, a review summarized all the physical treatments that showed a decrease in allergenicity (Kerezsi et al., 2022), another essential aspect determined by interactions within the protein structure.

Among the treatments discussed, microfluidization, or dynamic high-pressure microfluidization (DHPM), has emerged as an innovative technique that has attracted attention recently. It modifies macromolecules such as protein, starch, dietary fiber, and non-starch polysaccharides, influencing their particle size, solubility, antioxidant activity, and emulsifying properties (Guo et al., 2020). Besides the techno-functional properties that can be modified, this method also investigated allergens in different foods, such as peanuts or milk (Y. Chen et al., 2016; C. Qiu Hu et al., 2011). For example, following a 60 MPa microfluidization treatment, Ara h 2 (the main allergen in peanuts) experienced changes in the secondary structure. The percentages of α-helices and β-turns notably decreased, while the percentage of β-sheets increased, all correlated with a decrease in the antigenicity of peanuts (C. Qiu Hu et al., 2011).

Furthermore, microfluidization combines various forces such as high pressure, high-velocity impacts, high-frequency vibrations, instantaneous pressure drops, high shear forces, turbulence, and hydrodynamic cavitation phenomena to disrupt the structure of the treated components. In the context of proteins, microfluidization disrupts protein aggregates, enhances solubility, and modifies protein structures (Guo et al., 2020). The shape of the geometrical chamber (Z or Y type), diameter, number of passes, temperature, pressure, and the nature of the treated sample are the most essential treatment conditions to have an efficient process (Li et al., 2022).

Therefore, different researchers studied the impact of microfluidization on the soybean protein structure. For instance, SPI was treated at 120 MPa for 3 passes, and an increase in surface hydrophobicity, solubility, and disulfide bonds were observed. Also, stability against creaming and emulsifying efficiency were improved. Related to protein structure, this treatment disrupted the insoluble aggregates into small solubles, unfolded and denatured the proteins (Shen & Tang, 2012). Research on edible birds' nests recently revealed that water-insoluble protein fraction experienced partial solubilization (26–27 %) following microfluidization treatment at 120 MPa. This increase in solubility could be linked not only to the reduction in particle size but also to the modifications in the protein's secondary structure (increase in α-helix 11.63 % (0 MPa) to 13.43 % (120 MPa) (Chok et al., 2021). Microfluidization can also be applied to other proteins, resulting in a modified structure for peanut protein isolate, ovalbumin, β-lactoglobulin, pea globulin, potato protein isolate, and more. A recent review (Ozturk & Turasan, 2021) described the latest developments in the applications of microfluidization with an overview of research articles using this technique on protein structure.

To our knowledge, no investigations have yet considered the impact of microfluidization on the secondary structure of soybean protein isolate by combining different numbers of passes with or without controlling the temperature during the process. Consequently, this article describes the effect of the microfluidization process on the structural aspect of soybean protein isolate, both in its powdered and liquid forms. Moreover, it differentiates the impact of heat induced during shearing and pressure by testing different parameters regarding the number of passes and temperature. The paper focuses on mid-infrared and fluorescence spectroscopy techniques.

2. Material and methods

2.1. Materials

Soybean protein isolate was purchased from SEAH International (France). The protein content is 90.0 % (not related to the dry matter). It was determined by the Dumas method (N × 6.25), according to Serrano et al., 2013 and using Elementar (Rapid N Exceed). 1-anilinonaphthalene-8-sulfonic acid (ANS) was used to assess protein surface hydrophobicity (PSH) and it was obtained from Cayman Chemical Company (supplier − Sanbio B.V, Netherlands).

2.2. Processing

Microfluidization treatment

A 5 % w/v protein solution of SPI was prepared by dispersing SPI in Milli-Q ultrapure water at neutral pH (close to 7). The solution was stirred for 4 h at ambient temperature (25 °C) and left overnight at 4 °C for complete hydration. Subsequently, the SPI solution was subjected to microfluidization treatment Microfluidizer Processor M−110EH from Microfluidics International Corporation. As we used a pilot scale process, the solution was adapted to this condition.

During this treatment, the liquid was pumped through two interaction chambers composed of a fixed geometry chamber (Z-type) — the first chamber having 200 μm, followed by the second with 100 μm (Fig. 1). The microfluidization was conducted with and without temperature control during the process, the solutions being treated at a pressure of 137 MPa. The solutions prepared were circulated in the system for 1, 3, or 5 passes.

During processing with the cooling system, temperature regulation was achieved using a heat exchanger (SC5000 Recirculating cooler, JULABO GmbH), where the temperature was set at 10 °C. The samples where the cooling system was applied are named 1PW, 3PW, and 5PW, where 1, 3, and 5 represent the number of passes used for this treatment. The microfluidized samples where the temperature was not controlled were also denoted as 1PN, 3PN, and 5PN.

A non-microfluidized sample was used as a control for the following experiments, named "C.".

Frozen solutions from microfluidization treatment were freeze-dried (Christ Gamma 2–16 LSC Plus) for 96 h. Primary and secondary desiccations were performed during 72 and 24 h under 1.00 and 0.005 mbar pressures. Freeze-dried samples were ground until a homogeneous powder was obtained and stored at 15 °C before analysis.

2.3. Sample analysis

Because we were interested in the behavior of the proteins for the

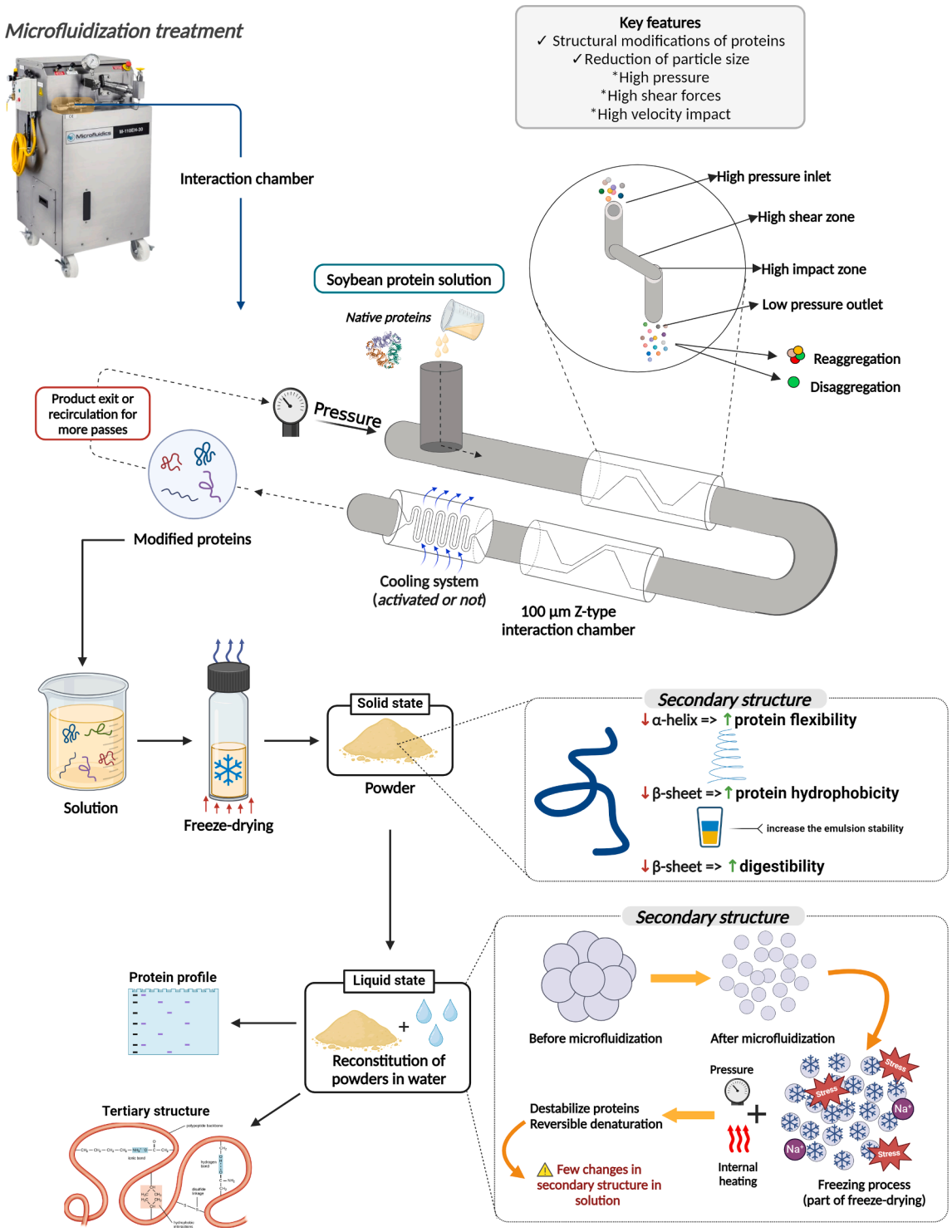

Fig. 1. Schematic representation of the microfluidization process, focusing on the Z-shaped interaction chamber design (Microfluidics) (Created with BioRender.com).

secondary structure, the following sections will focus on contrasting the mentioned samples in their different states; either as a powder or as a liquid.

The microfluidized powders obtained after freeze-drying and the control were used in their initial state to elaborate the secondary structure.

Microfluidized powders and control were also used to reconstitute liquid samples in Milli-Q ultrapure water for a final 5 % protein solution (w/v) concentration. The solutions were stirred for 2 h at 250 RPM, maintaining an ambient temperature of 25 °C at their natural pH (close to 7). These solutions were designed to analyze the secondary structure, intrinsic fluorescence, and protein surface hydrophobicity. To analyze the primary structure, 20 mg of samples were solubilized with 1 mL of Tris-SDS buffer for 2 h at room temperature.

2.3.1. Sodium dodecyl sulfate polyacrylamide gel electrophoresis (SDS-PAGE)

Proteins were separated according to Laemmli (1970) using 5 %

stacking gel and 12 % separating gel (Blancher & Jones, 2001). Protein samples were solubilized in Tris-SDS buffer, containing 4 % (w/v) SDS, 10 mM Tris HCl (pH = 7.4), and protease inhibitor. They were quantified using the DC Protein assay kit for microplates. After protein solubilization and quantification, the samples were heated for 10 min at 70 °C. Then, 20 μL of the solution was loaded per well, having 20 μg of proteins. Electrophoresis under reducing conditions was performed at room temperature at a constant voltage of 60 V for 30 min, followed by 90 min at 120 V. Precision Plus Protein Unstained Protein Standards, Bio-Rad (250–10 kDa) was used to estimate protein size. After electrophoresis, the gels were stained in a Silver Blue solution for one night. The gels were read using the ChemiDoc MP imaging system and analyzed by the Image Lab 6.1 Software, both from Bio-Rad Laboratories.

2.3.2. Mid-infrared (MIR) measurement in powder and solution

The soybean protein secondary structure was analyzed using the Fourier Transform Infrared Spectroscopy (FTIR) method on the spectrometer IRTracer-100 (Shimadzu, Duisburg, Germany). The analysis was performed on powders and solutions described in the previous section.

The spectra of solutions and powders were recorded in a horizontal attenuated total reflectance (ATR) cell with zinc selenide crystal, using 20 reflections over the wavenumber range of 900 to 3000 cm^{-1}. Sixty-four scans were accumulated for each spectrum with a resolution of 16 cm^{-1}. Milli-Q ultrapure water was used as a background for the solutions analysis, and air for the powders. The second derivative analysis was applied to the MIR spectra for the amide I, II, and III regions to quantify the secondary structure proportions. The analysis was performed in triplicate for both powders and solutions. LabSolutionIR software (Easy Macro function) determined the estimation of protein secondary structure.

2.3.3. Intrinsic fluorescence measurement in the solution

The intrinsic fluorescence of the solutions at their natural pH was determined using a Fluoromax-4 spectrofluorometer (Jobin Yvon, Horiba, NJ, USA) equipped with a temperature controller (T Haake A25 AC200) and a thermostatically controlled quartz cell. The analysis was carried out at 25 °C, based on the method of (Nahimana et al., 2023), with slight modifications for the protein concentration. For this study, we used 2 ml of the 5 % protein solutions (w/v), incubating for 3 min in a dark place. The excitation wavelength was set for 290 nm and 305–450 nm for emission. The analysis was performed in triplicate.

2.3.4. Protein surface hydrophobicity (PSH)

The protein surface hydrophobicity of the microfluidized samples was evaluated by using a Fluoromax-4 spectrofluorometer (Jobin Yvon, Horiba, NJ, USA) equipped with a temperature controller (T Haake A25 AC200) and a thermostatically controlled quartz cell. The samples were treated with ANS − solution (8 mM) as a fluorescence probe in different concentrations (0 to 150 μM). Depending on the concentration, 5 μl or 7.5 μl of ANS was added to each 2 ml of the 5 % protein solutions (w/v), incubating for 3 min in a dark place. The excitation wavelength was configured at 290 nm, while the emission range was between 305 and 450 nm. The analysis was performed in triplicate. The PSH of the samples was calculated using the Lineweaver-Burk equation:$1/F = 1/F_{max} + Kd/[ANS] \times F_{max}$, which is explained by (Miriani et al., 2011), and it is expressed in if/g × μM. After calculating all the parameters, PSH was determined by the formula $PSH = [F_{max}/ Kd]/[P]$. In the following paragraph, each element of the equation is individually outlined.

F: the maximum registered fluorescence intensity observed due to the binding of ANS to the hydrophobic surface sites of proteins.

F_{max}: the maximum fluorescence that can be achieved under ANS saturated concentration and, therefore, the maximum number of binding sites where ANS could bind.

ANS: concentration of ANS expressed in μM.

Kd: apparent dissociation constant of a supposed monomolecular complex (protein-ANS) expressed in μM.

P: protein concentration in the solution (g/L).

2.3.5. Statistical analysis

Statistical analysis was performed with IBM SPSS Statistics (V 28, 2021). All data were analyzed using univariate analysis, and differences between means were evaluated using the Tukey test with a p-value < 0.05 for significant differences.

3. Results and discussion

3.1. Impact of microfluidization on the primary structure of soybean protein isolate

SDS-PAGE was performed to analyze the molecular weight distribution of the native and microfluidized SPIs. Fig. 2 shows the electrophoretic profile obtained after the treatment, and the proteins based on their size were identified from the literature (J. Wang et al., 2022; L'Hocine & Boye, 2007).

SDS-PAGE under reducing conditions showed that the protein bands remained unchanged when exposed to microfluidization treatment, indicating no protein fragmentation. This phenomenon was previously observed for whey and hazelnut proteins (Saricaoglu et al., 2018; Bouaouina et al., 2006). These results suggest that microfluidization does not impact the primary structure of soy proteins, which is consistent with the literature (Gong et al., 2019; H. Chen et al., 2019).

After electrophoresis, different proteins were detected in our native and microfluidized SPIs: the α' subunit (≈ 76 kDa), α subunit (≈ 72–74 kDa), and β subunit (≈ 48–50 kDa) of β-conglycinin (Gly m 5); the acidic chain (≈ 33–40 kDa) and basic chain (≈ 20–22 kDa) of glycinin (Gly m 6); the Kunitz trypsin inhibitor (≈ 20 kDa) and the pathogenesis-related protein (≈ 17 kDa) (Gly m 4). Other minor bands were identified corresponding to the P34 soybean vacuolar protein (≈ 30–34 kDa) (Gly m Bd 30 K), 2S albumin Gly m 8 (≈ 28 kDa), and 7S globulin Gly m Bd 28 K (≈ 26 kDa). Moreover, according to the literature, the bands presented at the top of the gel and those > 150 kDa seem to be aggregates (J. Hu et al., 2023; Shen & Tang, 2012). Finally, it is also interesting to notice that the SDS-PAGE profiles did not allow Gly m 1 (hydrophobic protein) and Gly m 2 (defensin) to be observed. Both hull proteins might be removed during dehulling (L'Hocine & Boye, 2007). Additionally, all the mentioned proteins are responsible for soybean allergy.

3.2. Mid-infrared analysis

3.2.1. Mid-infrared spectra

Mid-infrared (MIR) spectroscopy provides insight into the characteristic vibration patterns of covalent bonds within molecules. As a result, it offers quantitative data about all the components, including proteins, that can absorb IR radiation (Etzion et al., 2004). Also, it provides information about the changes in protein structure (T. Zheng et al., 2019).

To assess the impact of the microfluidization process with and without temperature control on the SPI secondary structure under different cycles, we conducted MIR spectroscopy scans within the range of 3000–900 cm^{-1}. FTIR-ATR spectra are divided into 3 regions, which correspond to fat (3,000–2,800 cm^{-1}), protein (1,700–1,500 cm^{-1}), and fingerprint (1,500–900 cm^{-1}) (Boubellouta & Dufour, 2012). The results of this method are presented in Fig. 3 (a), (b) for the powders, and Fig. 4 (a), (b) for the solutions, where different major bands were found.

According to Türker-Kaya & Huck, 2017, an essential peak for determining the secondary structure of proteins in the MIR spectrum is the amide I band, between 1650 and 1630 cm^{-1} (C = O stretching vibration), followed by the amide II, which contains mainly protein in the range of 1560 − 1540 cm^{-1} (N–H stretch and C = N). In plants, lignin, cell wall polysaccharides, protein, and lipids can be observed between

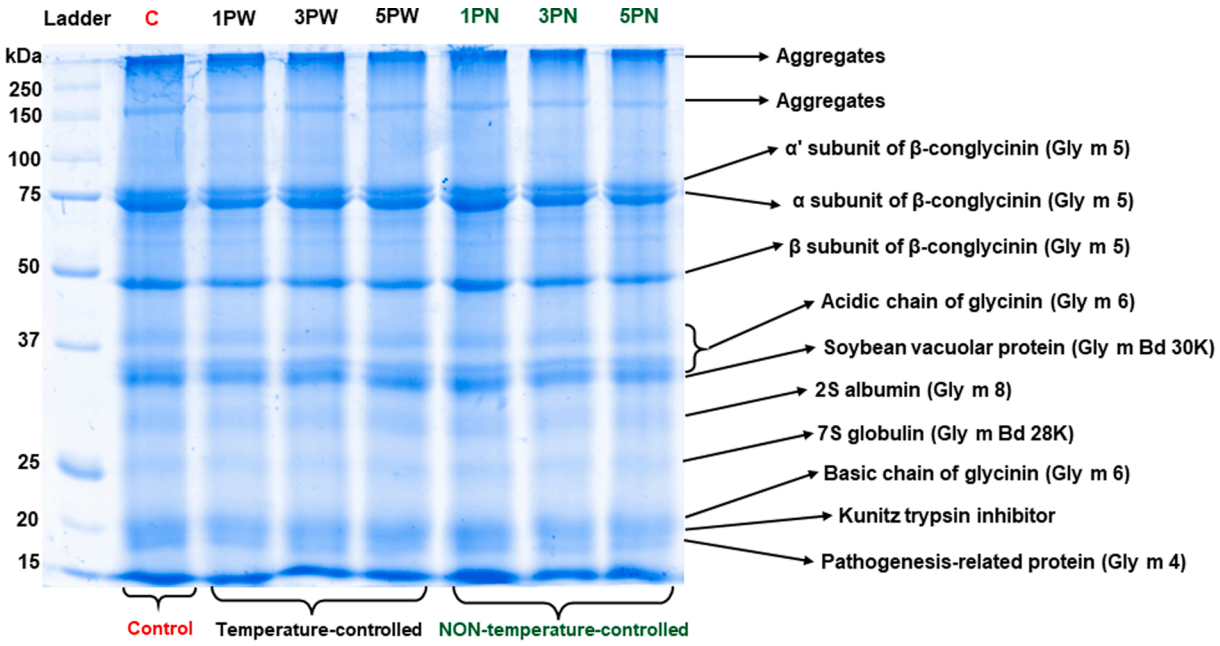

Fig. 2. SDS-PAGE profile under reducing conditions of native and microfluidized SPIs. Lane 1: standard marker. Lane 2 represents the non-treated SPI as a control. Lanes 3, 4, and 5 indicate the microfluidized samples where the temperature was controlled. Lanes 6, 7, and 8 refer to the microfluidized samples without temperature control.

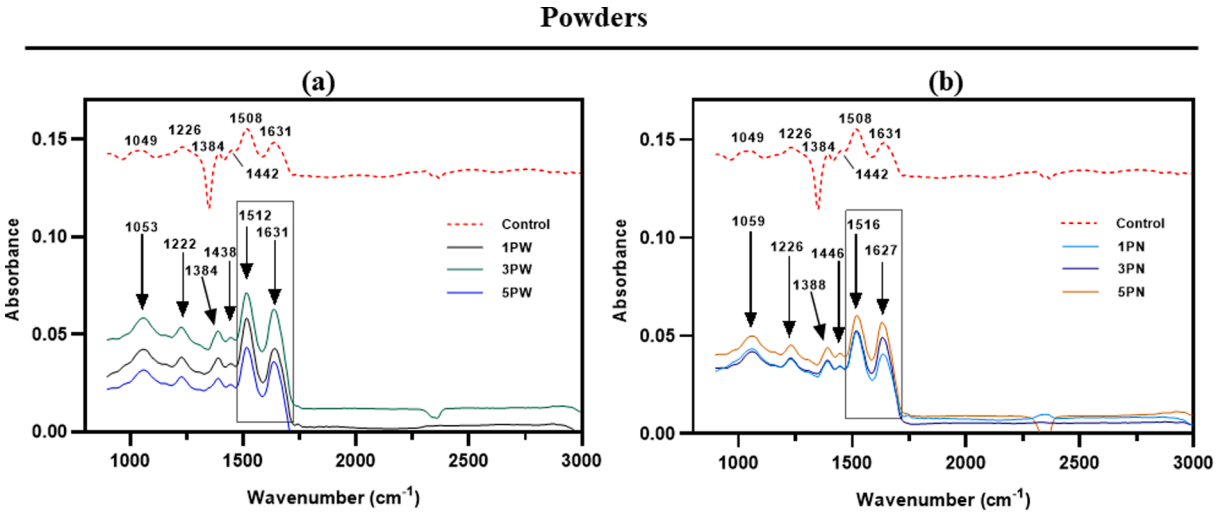

Fig. 3. Mid-infrared spectra of native and microfluidized SPIs in the powder. The spectral region considered in this study is from 900 to 3000 cm^{-1}. Microfluidized samples where temperature is controlled are represented by (a) and without a temperature controlled by (b).

1515 and 1150 cm^{-1} (C–H asymmetric and symmetric bending, C = C aromatic stretch, C–O) (Türker-Kaya & Huck, 2017).

The peaks associated with the secondary structure are linked to α-helix (1650–1660 cm^{-1}), β-sheet (1620–1641 cm^{-1}), β-turn (1660–1690 cm^{-1}), random coil (1641–1650 cm^{-1}), aggregates A1 (1610–1620 cm^{-1}) and A2 (1690–1695 cm^{-1}). Aggregates A1 and A2 represent the intermolecular and intramolecular between β-sheets (Long et al., 2015; Carbonaro & Nucara, 2010).

In the following sections, we present the spectra obtained in MIR for the microfluidized samples in both states – powder and solution and the band assignments for the different regions.

3.2.1.1. Protein as a dry powder – spectra analysis of microfluidized SPI, with and without temperature-controlled. The bands found within the range of 3,000 to 2,800 cm^{-1}, which are linked to C–H stretching vibration, are recognized for their sensitivity to the physical condition of lipids (Boubellouta & Dufour, 2012). The absence of the peak in this region (Fig. 3 (a) and (b)) illustrates the very low amount of fat in our samples.

For the microfluidized powders where the temperature is controlled (Fig. 3 (a)), the prominent peak observed related to proteins is 1631 cm^{-1} (C = O stretching). This is assigned to the β-sheet, corresponding to a low-frequency range (Carbonaro & Nucara, 2010). According to Pelton & McLean, 2000, the peak observed at 1512 cm^{-1} belongs to Amide II (CN stretching, NH bending) and is a structure of the antiparallel β-sheet. The same trend was noticed for the microfluidized powders where the temperature was not controlled (Fig. 3 (b)). β-sheet is observed at 1627 cm^{-1} (C = O stretching) and antiparallel β-sheet at 1516 cm^{-1} (CN stretching, NH bending). Moreover, when the control is compared with the microfluidized powders, it can be observed that the

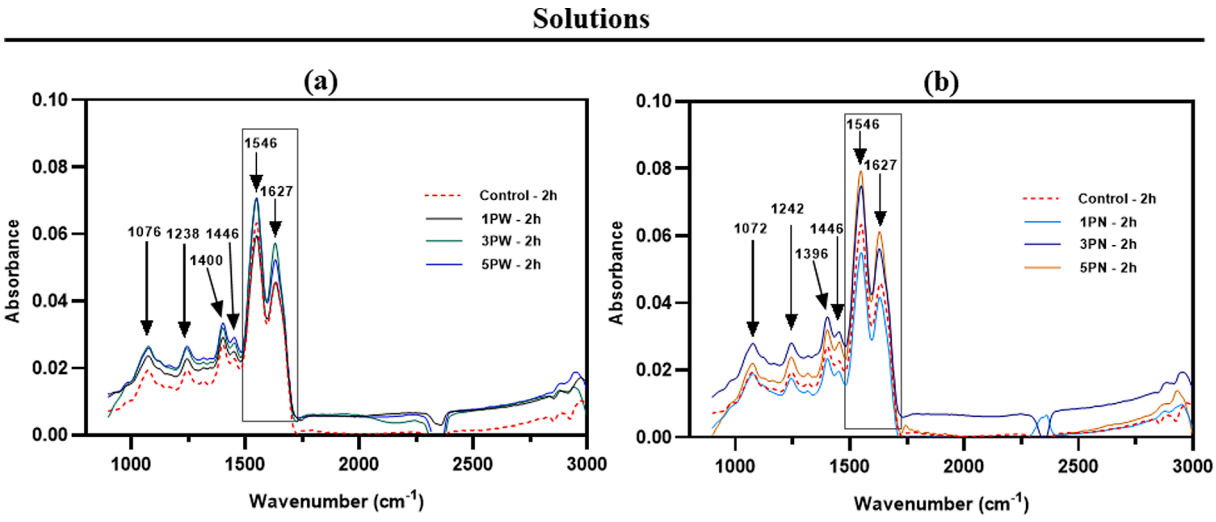

Fig. 4. Mid-infrared spectra of native and microfluidized SPIs in the solution. The spectral region considered in this study is from 900 to 3000 cm^{-1}. Microfluidized samples where temperature is controlled are represented by (a) and without a temperature controlled by (b).

absorbance is about 3 times higher.

The small peaks represent the low fingerprint contamination of the samples. In addition, the two highest peaks correspond to the high amount of protein present in the SPI.

3.2.1.2. Solubilized protein – spectra analysis of microfluidized SPI, with and without temperature-controlled. Regarding the samples in their liquid form (Fig. 4 (a) and (b)), the findings obtained showed a similarity in the case of both conditions (with and without controlling the temperature) when compared with the control. The peak corresponds to the β-sheet absorbed at 1627 cm^{-1} (C = O stretching) in the Amide I region. In the amide II region of the spectrum, a parallel β-sheet structure was found at a higher frequency of 1546 cm^{-1}. The graphs show that when the powders are reconstituted in water, the absorbance is similar for all the samples, including the control. The protein tends to adopt more energetically stable conformations as the water content increases. This might occur because of the increased mobility of protein segments and the occupation of empty spaces within these configurations (Abbott et al., 1996).

Also, in this case, the small peaks represent the low fingerprint contamination of the samples, and the two highest peaks correspond to the high amount of protein present in the SPI.

The findings presented for the solid and liquid forms provided information regarding the SPIs during high-intense shear treatment, allowing us to visualize the structural changes of the protein.

3.2.2. Secondary structure analysis

The second derivative analysis was applied to study the changes in the soybean protein structure. This analysis determined the percentages of α-helix, β-sheet, β-turn, random coil, aggregates A1, and aggregates A2, presented in Tables 1, 2, 3, and 4.

Thus, the following sections will present different properties of the protein linked to their secondary structure. These will be related to the techno-functional properties (L. Zheng et al., 2021; Djemaoune et al., 2019), allergenicity (Pi et al., 2021; Jideani, 2011), digestibility (Melchior et al., 2022; Pan et al., 2022; Carbonaro et al., 2012) and flexibility of proteins (Yan et al., 2021; Zhu et al., 2020).

3.2.2.1. Protein as a dry powder – spectra analysis of microfluidized with temperature-controlled SPI. Table 1 presents the percentages of protein secondary structure for the SPIs microfluidized powders where the temperature is controlled. Compared to the control, we notice that the SPI treated by microfluidization showed a significant decrease in the quantities of β-sheet and random coil ($p < 0.05$). Moreover, it is not the same trend for α-helix, which has a slight reduction. On the other hand, the proportions of β-turn, A1, and A2 aggregates increased significantly ($p < 0.05$).

Interestingly, it was also observed that the most significant changes ($p < 0.05$) are for β-sheet, the proportion decreasing from 20.03 % for native SPI (control) to 15.40 %, 9.00 %, and 8.43 % for 1, 3, and 5 passes, respectively. This reduction can have an impact on protein properties such as digestibility. Carbonaro et al., 2012 demonstrated an inverse correlation between the proportion of β-sheet and protein digestibility. In this case, decreasing the β-sheet ratio could increase their digestibility. This could also impact the allergenicity. Related to this, different researchers explained that an increase in digestibility could be linked with a reduction in allergenicity during the digestive process (H. Chen et al., 2019; Rahaman et al., 2016; Zhong et al., 2014).

The observed decrease in β-sheet and the increase in β-turns in treated samples indicated that microfluidization may lead to protein unfolding, with the hydrophobic regions opening and becoming exposed (Fang et al., 2020). This will increase the protein hydrophobicity, which is detailed in the following section.

Furthermore, another aspect impacted by microfluidization is related to the α-helix. A decrease in the α-helix was observed for the microfluidized SPIs and can be connected with increased flexibility.

Table 1
Secondary structure (%) of the native and microfluidized treated SPI (controlling the temperature) in the powder.

Sample	α-helix	β-sheet	β −turn	Random coil	Aggregates A1	Aggregates A2	A1 + A2
C	8.93 ± 0.15^{c}	20.03 ± 0.21^{e}	38.67 ± 0.06^{a}	11.87 ± 0.06^{e}	15.13 ± 0.06^{a}	5.37 ± 0.06^{a}	$20.50 \pm 0.12^{a,b}$
1PW	8.17 ± 0.06^{a}	15.40 ± 1.61^{d}	40.63 ± 0.86^{b}	$10.20 \pm 0.10^{c,d}$	19.27 ± 0.25^{c}	6.40 ± 0.56^{b}	$25.67 \pm 0.81^{c,a,b}$
3PW	8.40 ± 0.00^{a}	9.00 ± 0.79^{b}	45.80 ± 0.17^{c}	8.57 ± 0.12^{a}	20.43 ± 0.25^{d}	7.73 ± 0.32^{c}	$28.17 \pm 0.57^{d,b}$
5PW	8.23 ± 0.06^{a}	8.43 ± 0.90^{b}	46.03 ± 0.06^{c}	8.37 ± 0.15^{a}	21.00 ± 0.40^{d}	7.97 ± 0.40^{c}	$28.97 \pm 0.80^{d,\ b}$

The data refers to the mean ± standard deviation of triplicate measurements. Values in the same column with different superscripts (a-e) represent significant differences ($p < 0.05$) between the treated and non-treated samples.

Table 2
Secondary structure (%) of the native and microfluidized treated SPI (without controlling the temperature) in the powder.

Sample	α-helix	β-sheet	β −turn	Random coil	Aggregates A1	Aggregates A2	A1 + A2
C	8.93 ± 0.15^{c}	20.03 ± 0.21^{e}	38.67 ± 0.06^{a}	11.87 ± 0.06^{e}	15.13 ± 0.06^{a}	5.37 ± 0.06^{a}	$20.50 \pm 0.12^{a,b}$
1PN	8.67 ± 0.06^{b}	11.53 ± 0.38^{c}	45.57 ± 0.21^{c}	10.00 ± 0.10^{c}	17.00 ± 0.00^{b}	7.17 ± 0.12^{bc}	$24.17 \pm 0.12^{b,ab}$
3PN	9.17 ± 0.15^{c}	3.73 ± 0.06^{a}	51.57 ± 0.12^{d}	9.63 ± 0.21^{b}	16.87 ± 0.12^{b}	9.10 ± 0.00^{d}	25.97 ± 0.12^{c}
5PN	9.53 ± 0.06^{d}	3.87 ± 0.06^{a}	52.43 ± 0.06^{d}	10.37 ± 0.06^{d}	14.70 ± 0.10^{a}	9.10 ± 0.00^{d}	23.80 ± 0.10^{b}

The data refers to the mean ± standard deviation of triplicate measurements. Values in the same column with different superscripts (a-e) represent significant differences ($p < 0.05$) between the treated and non-treated samples.

Table 3
Secondary structure (%) of the native and microfluidized treated SPI (controlling the temperature) in the solution.

Sample	α-helix	β-sheet	β −turn	Random coil	Aggregates A1	Aggregates A2	A1 + A2
C-2 h	9.07 ± 0.06^{a}	21.53 ± 0.32^{bc}	36.70 ± 0.10^{a}	13.40 ± 0.10^{a}	14.30 ± 0.30^{b}	5.00 ± 0.10^{ab}	19.30 ± 0.40^{b}
1PW-2 h	9.13 ± 0.06^{ab}	21.83 ± 0.15^{d}	36.70 ± 0.20^{a}	13.50 ± 0.10^{a}	14.03 ± 0.06^{ab}	4.83 ± 0.06^{a}	18.86 ± 0.12^{ab}
3PW-2 h	9.37 ± 0.06^{bc}	20.27 ± 0.12^{a}	37.77 ± 0.12^{c}	13.40 ± 0.10^{a}	14.03 ± 0.06^{ab}	5.17 ± 0.06^{b}	19.20 ± 0.12^{b}
5PW-2 h	9.23 ± 0.06^{bc}	21.10 ± 0.17^{b}	36.90 ± 0.00^{ab}	13.53 ± 0.15^{ab}	14.23 ± 0.15^{b}	5.03 ± 0.06^{ab}	19.26 ± 0.21^{b}

The data refers to the mean ± standard deviation of triplicate measurements. Values in the same column with different superscripts (a-d) represent significant differences ($p < 0.05$) between the treated and non-treated samples.

Table 4
Secondary structure (%) of the native and microfluidized treated SPI (without controlling the temperature) in the solution.

Sample	α-helix	β-sheet	β −turn	Random coil	Aggregates A1	Aggregates A2	A1 + A2
C-2 h	9.07 ± 0.06^{a}	21.53 ± 0.32^{bc}	36.70 ± 0.10^{a}	13.40 ± 0.10^{a}	14.30 ± 0.30^{b}	5.00 ± 0.10^{ab}	19.30 ± 0.40^{b}
1PN-2 h	9.17 ± 0.06^{ab}	21.40 ± 0.35^{bc}	37.10 ± 0.26^{ab}	13.47 ± 0.06^{a}	13.97 ± 0.12^{ab}	4.93 ± 0.06^{a}	18.90 ± 0.18^{ab}
3PN-2 h	9.27 ± 0.06^{bc}	21.17 ± 0.35^{bc}	36.93 ± 0.12^{ab}	13.80 ± 0.10^{b}	13.80 ± 0.00^{a}	5.00 ± 0.10^{ab}	18.80 ± 0.10^{ab}
5PN-2 h	9.23 ± 0.06^{c}	21.37 ± 0.21^{bc}	37.17 ± 0.21^{b}	13.60 ± 0.00^{ab}	13.70 ± 0.10^{a}	4.93 ± 0.06^{a}	18.63 ± 0.16^{a}

The data refers to the mean ± standard deviation of triplicate measurements. Values in the same column with different superscripts represent (a-c) significant differences ($p < 0.05$) between the treated and non-treated samples.

According to Tang, 2017, flexibility is related to how proteins adapt to changes in their external environment, affecting soy proteins' emulsion stability. In this way, a lower amount of α-helix suggests a higher protein flexibility (Zhu et al., 2020).

If the number of cycles is compared, we can notice a significant difference ($p < 0.05$) between the SPI passed 1 and 3 times (when the temperature is controlled) for all secondary structures (except for α-helix). However, no significant differences were observed between 3 and 5 passes for any of the secondary structures studied. This suggests that the changes during microfluidization treatment depend on the number of passes and the heating resulting from the shearing effect. It seems that 1 or 3 passes are enough to see a modification in the secondary structure. At higher passes, the resulting mechanical forces might be responsible for the protein rearrangement and aggregation, forming new electrostatic interactions and disulfide bonds (Melchior et al., 2022).

3.2.2.2. Protein as a dry powder – spectra analysis of microfluidized without temperature-controlled SPI. Similar trends are observed for microfluidization treatment without controlling the temperature but with a few differences (Table 2). When microfluidization is applied for the SPIs and the temperature is not controlled, there is a significant decrease in β-sheet and an increase in β-turn ($p < 0.05$). A minor decrease in random coil content was observed, while A2 increased with the number of passes (between 1 and 3, but not for 5). Regarding the impact of temperature, when this is not controlled, it increases with each pass. In this way, after 1 pass, the temperature reached was close to 42 °C, then increased to 65 °C after 3 passes, and it ended with 75 °C passing 5 times in the microfluidizer.

On the other hand, the data for α-helix showed a different trend from the one observed in the treatment where the temperature was controlled. The increase of the internal heating can explain the increase in α-helix for 3 and 5 passes due to the shearing effect, and this was demonstrated when heat treatment was applied to soy proteins (T. Li et al., 2021; Long et al., 2015; Carbonaro et al., 2012). Considering the information described above regarding the flexibility of proteins (Zhu et al., 2020), it seems that 3 and 5 passes are less suitable for forming a stable emulsion.

Moreover, it has also been demonstrated that applying heat treatment to soy proteins increases the proportions of β-turn and A2 aggregates and decreases β-sheet proteins. These results were also obtained for the heat treatment at 65 °C and 75 °C for 1 h (T. Li et al., 2021; Long et al., 2015; Carbonaro et al., 2012), compared with microfluidization treatment, were for 5 passes were registered around 46 min (flow rate 26 l/h). It was observed that both temperature and shearing treatment contribute to the modification of the structure when the cooling system is not used, leading to more significant changes in the proportions of these structures than using the cooling system. On the contrary, a decrease in A1 aggregates was shown when heat treatment was applied to soy proteins. This results in the unfolding of proteins and increased exposure of hydrophobic groups on their surfaces. These exposed hydrophobic groups can then interact, potentially forming aggregates. The unfolding of polypeptide chains and the formation of aggregates often happened simultaneously, indicating that these changes occurred at various levels (Long et al., 2015).

In the same way, as for microfluidization with the cooling system, there were no significant differences between 3 and 5 passes for most secondary structures. However, this is not the case for α-helix, random coils, and aggregates A1, where we have a statistical difference ($p < 0.05$). Furthermore, compared with the control, a drastic decrease can be observed for β-sheet for 3 and 5 passes, from 20.03 % to 3.73 % and 3.87 %, respectively. Similar findings are reported by Gong et al., 2019

for a pressure higher than 120 MPa. They explained that exposing the sample to 120 MPa resulted in the most significant disruption of the aggregated structure, and applying higher pressures led to a reformation of the aggregates.

Additionally, if we consider the results obtained by Y. Chen et al., 2016, treated samples 3PN and 5PN are potentially suitable for reducing soybean allergens. The researchers explained that decreasing in β-sheet and increasing in α-helix led to a notable improvement in binding capacity, resulting in a decrease in allergenic potential. However, the correlation between this protein's secondary structure and binding capacity requires more studies to prove if there is a relation between them.

3.2.2.3. Solubilized protein – spectra analysis of microfluidized with temperature-controlled SPI. The influence of microfluidization in the liquid samples with temperature control is presented in Table 3. Compared to the dry state, results show that the protein's secondary structure changes completely when the powders are reconstituted in water. These observations could be due to the hydrogen bond variation induced by pressure, the number of passes (Melchior et al., 2022), and/or the freeze-drying process (Arakawa et al., 2001). When microfluidization was applied, no significant difference was observed for α-helix, random coil, aggregates A1 and A2. However, a considerable difference was highlighted for β-sheet and β-turn. For α-helix, a slight increase from 9.07 % to 9.13 %, 9.37 %, and 9.23 % for 1, 3, and 5 cycles is observed when compared to the control. Regarding β-sheet, between the microfluidized samples, there is a significant difference ($p < 0.05$); the highest content of β-sheet is represented by one treatment cycle.

These results could be explained by the fact that protein molecules interact directly in the powders. Without the presence of excess bulk water molecules, intermolecular interactions become more energetically favorable. In contrast, after the reconstitution of the samples in water, the protein configuration changes, inducing reversible denaturation (Liao et al., 2002).

Further, after the hydration, the total number of aggregates (A1 + A2) is decreasing, and the content of β-sheet is increasing. This might be due to the disruption of the soluble aggregates, which are dissolved in water and then converted back to β-sheet. This observation can not be applied to the solid-state (see previous section), where is observed the opposite trend (increasing aggregates and decreasing in β-sheet). In this case, the interaction between β-sheets forms the aggregation phenomenon (Luo et al., 2022).

Lyophilization applied after the microfluidization treatment could also explain the difference in results compared with the solid state. Very interestingly, the lyophilization process alone can subject protein and peptide molecules to stress, causing considerable modifications in conformation when stabilizing excipients (such as sugars, sugar alcohols, surfactants, specific amino acids, buffers, and polymers) are absent (Thakral et al., 2021; Carpenter et al., 1997). One exciting aspect of these findings is that the interactions between proteins and sugars through hydrogen bonding are important for stabilizing proteins (Carpenter et al., 1992; Carpenter & Crowe, 1989).

Regarding stability, most proteins are quite delicate under neutral pH and room temperature conditions, making them easily susceptible to denaturation when subjected to temperature and pressure variations, changes in pH, and adding substances such as chaotropic salts, guanidine, HCl, or urea (Arakawa et al., 2001; Pace, 1990). Besides freeze-drying, freeze-thawing is also responsible for the stress described above. Many proteins are not stable to these, even if they are one of the most common methods for the long-term storage of proteins (Arakawa et al., 2001).

Furthermore, it is noteworthy that microfluidization can modify the structure of globular protein aggregates accompanied by a decrease in particle size (Shen & Tang, 2012; Liu et al., 2011; Dissanayake & Vasiljevic, 2009). This size reduction will make more molecules available, which will be subjected to additional stress due to the formation of ice crystals. This process will form ice-water and ice-air interfaces, which can destabilize the protein. Additionally, the solution will become more concentrated when removing water (as ice), possibly altering the samples' pH, viscosity, and ionic strength (Thakral et al., 2021).

3.2.2.4. Solubilized protein – spectra analysis of microfluidized without temperature-controlled SPI. Results for the liquid samples without temperature control are presented in Table 4. The samples in their liquid state have a similar behavior in the spatial structure of the protein as samples where the temperature was controlled. However, it seems that β-sheet and β-turn are not changed during the reconstitution in water (no statistical differences). Interestingly, the intrinsic heat produced by the high shear and cavitation is responsible for this modification in the structure.

Furthermore, a difference between 1 and 5 cycles ($p < 0.05$) is observed for α-helix. Compared with the control, α-helix is increasing from 9.07 % to 9.17 %, 9.27 %, and 9.23 % for 1, 3, and 5 passes, respectively. C. Wang et al., 2020 reported that a slight increase in α-helix might be due to the complete solubilization of the proteins under the microfluidization treatment. Moreover, after the hydration, we can observe the same trend for the aggregates and β-sheet. The total number of aggregates is lower than the β-sheet, which is higher. This observation is due to the disruption of the soluble aggregates, which are dissolved in water and then converted back to β-sheet (Luo et al., 2022).

Similar to the samples obtained with temperature control, lyophilization might explain the difference in results by adding additional stress related to the formation of ice crystals and their consequences.

Finally, differences in the behavior of the protein in solid and liquid states are observed. By changing their conformation, the freeze-drying process seems to impact the treated samples when reconstituted in water. Moreover, microfluidization also contributed to the difference between the two states (powder and solution) by decreasing the particle size and opening more sites.

3.3. Intrinsic fluorescence spectra analysis

Fluorescence spectra analysis is a valuable technique that elucidates the changes in the tertiary structure of proteins, such as folding-unfolding and dynamics. Intrinsic fluorescence means the aromatic amino acids from proteins, such as tryptophan, tyrosine, and phenylalanine residues, have natural fluorescence that can signal protein conformational changes. Tryptophan gives the highest intensity when compared with the other mentioned aromatic amino acids, which is why it is most used in the intrinsic fluorescence methods (He et al., 2021; Vera et al., 2019; Turoverov & Kuznetsova, 2003). The maximum emission wavelength (λ_{max}) and the difference in the fluorescence intensity (FI) are the parameters to evaluate the modifications occurring in the proteins' tertiary structure (Nahimana et al., 2023).

3.3.1. Intrinsic fluorescence spectra analysis of microfluidized with temperature-controlled SPI in the solution

Fig. 5 presents the results of the maximum emission wavelength and the difference in the fluorescence intensity for the microfluidized SPI, where the temperature was controlled. As we can observe, the λ_{max} of the non-treated sample is 377 nm. The variation of microfluidized samples slightly increased for 1 and 3 passes (377.67 nm for both). If they are compared together, there is no difference between 1 and 3 passes. The highest number of passes (5) led to a higher emission wavelength of 378 nm. However, there is no statistical difference between the samples treated under this condition, except between 5PW and 3PN, which can be due to the high shear forces. A similar λ_{max} was observed for the white lupin protein isolate (Nahimana et al., 2023). When a pretreatment at 95 °C was applied before microfluidization for soybean protein isolate, the maximum emission wavelength was 337.4 nm, indicating an increase in hydrophilicity in the microenvironment

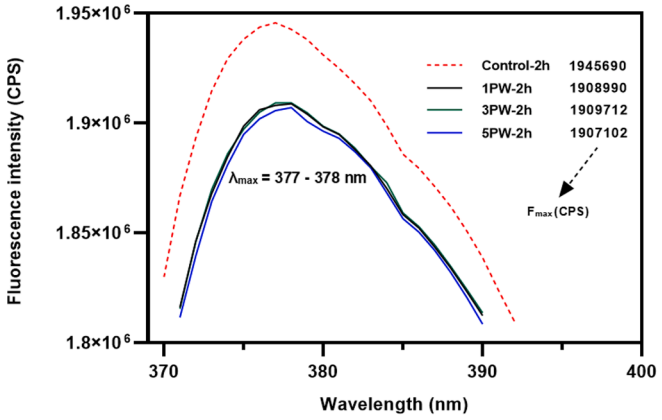

Fig. 5. Intrinsic tryptophan emission spectra of microfluidized samples at 137 MPa in the solution, where the temperature was controlled for 1, 3, and 5 passes compared to the non-treated SPI.

surrounded by tryptophan chromophores (Shen & Tang, 2012). The observed increase in maximum emission wavelength for our samples could also suggest that the microenvironment of the tryptophan becomes more hydrophilic with an increased number of passes. It signifies an increasing polarity around tryptophan residues caused by the unfolding of the protein and an enhanced interaction of the fluorophore with the aqueous medium (He et al., 2021; Ling et al., 2019).

On the other hand, when we look at the maximum fluorescence (F_{max}) for the 1PW, 3PW, and 5PW, F_{max} is decreasing compared with the control (Fig. 5). In our case, cross-linking of protein molecules might be responsible for the reduced fluorescence intensity, which indicating that tryptophan residues are less exposed for 5 passes (Ling et al., 2019). These findings suggest that the emission wavelength slightly increases and the fluorescence intensity decreases differently for each number of passes. Moreover, when microfluidization is applied, we observe modifications in the tertiary structure.

3.3.2. *Intrinsic fluorescence spectra analysis of microfluidized without temperature-controlled SPI in the solution*

The obtained results are different in the samples where the temperature was not controlled during the microfluidization treatment. As we can observe in Fig. 6, the λ_{max} increases after 1 pass (378 nm) compared to the non-treated SPI (377 nm). Moreover, there is a slight decrease for 3 passes (376.67 nm), and then for the most drastic treatment (5 passes), it returns at 377 nm. A statistical difference ($p < 0.05$) was noted between 1 and 3 passes, whereas this was not the case for the 5-pass cycle.

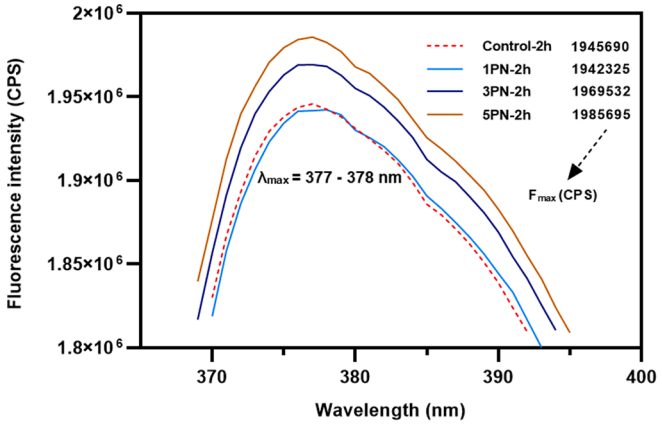

Fig. 6. Intrinsic tryptophan emission spectra of microfluidized samples at 137 MPa in the solution, where the temperature was not controlled for 1, 3, and 5 passes compared to the non-treated SPI.

Even if the temperature is increasing during the process (see materials and methods), due to the intrinsic high shear forces, the fact that the temperature is not controlled could be responsible for these oscillations in λ_{max}. The increase–decrease of the maximum emission wavelength was already described in the previous section (see 3.3.1.).

Interestingly, the results from the maximum fluorescence reveal the opposite compared to temperature-controlled samples. Namely, for 3 and 5 passes, F_{max} was increasing, compared to the control (Fig. 6). This result might be due to the protein unfolding caused only by high shear forces, cavitation, and pressure (Wu et al., 2019). In contrast, F_{max} decreased for one pass, which means a cross-linking or aggregation when soybean proteins are exposed to these conditions (Ling et al., 2019). If the samples are compared, we can assume that the F_{max} increases with the number of passes. Moreover, increased fluorescence intensity enhances the stability and emulsification properties (Zhu et al., 2020). Based on this, 3 and 5 passes without temperature control are suitable for further food applications. We also observe modifications in the tertiary structure configuration of soybean proteins for this treatment.

3.4. *Protein surface hydrophobicity*

Protein surface hydrophobicity evaluates different modifications in protein tertiary structure using ANS as an extrinsic fluorescence probe. Typically, ANS binds to exposed hydrophobic clusters within protein molecules. Consequently, PSH serves as an indicator of their surface hydrophobic characteristics, being essential for the functional properties of proteins, such as foaming, gelation, and emulsion (He et al., 2021; Z. Wang et al., 2014; Shen & Tang, 2012).

When the temperature was controlled, the PSH of the MF-treated samples showed an increased trend compared with the untreated SPI (1277.40 ± 31.89 if/g × μM). Surface hydrophobicity increases with the number of passes from 1307.54 ± 15.24 (if/g × μM) to 1490.45 ± 27.45 (if/g × μM) and 1986.29 ± 34.26 (if/g × μM) for 1, 3, and 5 passes, respectively. However, a significant difference ($p < 0.05$) was observed for the 3 and 5 cycles samples when they were compared with the non-treated sample (Fig. 7). These findings indicated that certain hydrophobic structural sections of treated SPI, such as hydrophobic amino acid residues, could become exposed after microfluidization due to the intense impact of high shear forces, high pressure, and cavitation. This exposure led to the dissociation of insoluble protein aggregates and protein unfolding (He et al., 2021; Fang et al., 2020). Another factor that may cause the increase in PSH can be related to the peptide chain expansion or the dissociation of the protein subunits or β-conglycinin denaturation (Z. Wang et al., 2014).

Furthermore, previous studies reported similar results, where PSH increased when samples were subjected to high-shearing treatment. For example, after exposing the peanut protein isolate to 210 MPa, the PSH increased by 2.2 times more than the control (Gong et al., 2019). Moreover, for pea albumin aggregates, it was found at 130 MPa, pH 7, that PSH increased and reached the maximum at this pressure (2.11 × 106 a.u) (Djemaoune et al., 2019). An increase in PSH was also observed for soybean protein isolate at 120 MPa – preheated and unheated samples (Shen & Tang, 2012).

On the other hand, compared with the non-MF sample (1277.40 ± 31.89 if/g × μM), an increase for the treated samples was observed for 1 (1441.02 ± 22.87 if/g × μM) and 3 passes (1485.96 ± 19.30 (if/g × μM) and a decrease for 5 passes (1217.28 ± 36.13 if/g × μM), if the temperature was not controlled. However, between 1 and 3 cycles, no significant difference was observed. The PSH of 5 cycles shows a statistical difference compared to 1 and 3 passes but remains similar to the control. This reduction may be attributed to the intrinsic heating formed naturally during the microfluidization treatment (Z. Wang et al., 2014). Also, the same authors reported that time, protein concentration, or temperature can influence the PSH.

To summarize, the order of increased surface hydrophobicity is as

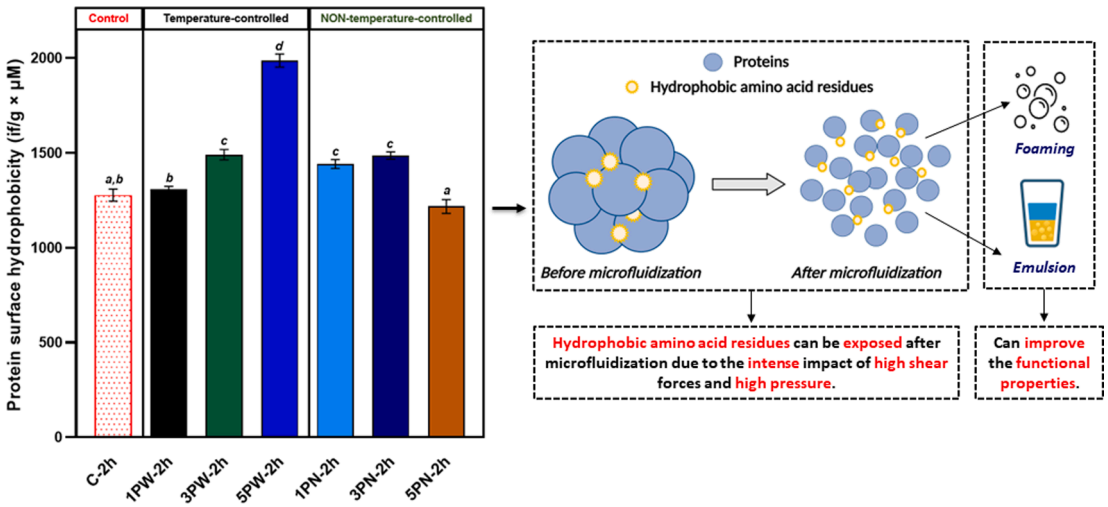

Fig. 7. The influence of microfluidization (137 MPa) on protein surface hydrophobicity at the natural pH of treated and non-treated soybean protein isolate. The data refers to the mean of triplicate measurements. Values in the column with different letters (a-d) represent significant differences ($p < 0.05$).

follows: 5PN-2 h < C-2 h < 1PW-2 h < 1PN-2 h < 3PN-2 h < 3PW-2 h < 5PW-2 h.

All the results show that microfluidization treatment impacts the tertiary structure of soybean proteins for specific conditions. These modifications could improve the functional properties, such as foaming or emulsifying.

3.5. Effect of temperature control and number of passes on soybean protein structures in microfluidization: A comparative analysis

This section presents an analysis to individually compare the effect of temperature control for 1, 3, and 5 passes, highlighting the differences in protein structures between passes with and without temperature control. Fig. 8 provides an overview of the comparative analysis. Results showed that all the samples presented a similar profile in the primary structure for the powder state. When comparing 1PW and 1PN, the difference in secondary structure was observed for almost all structural arrangements except random coil and A2. Additionally, for 3 and 5 passes, with and without temperature control, microfluidization influenced all secondary structure elements. The second group of microfluidized samples is related to their solution state. Analysis reveals no variation in the secondary structure between a single pass with and without temperature control. With 3 passes, differences were observed only in the β-sheet, β-turn, and random coil structures. Under more intense conditions with 5 passes, heating and multiple passes impact only the intermolecular interactions within β-sheets (A1). While no statistical difference was detected in the maximum emission wavelength among the samples, a significant difference ($p < 0.05$) was noted in the maximum fluorescence intensity for both 3 and 5 passes. Moreover, there was a difference in surface hydrophobicity between samples subjected to 1 and 5 passes. The results indicate that the internal heating produced by shearing and the number of cycles are essential to consider when selecting optimal parameters for specific protein structure modification. Furthermore, based on particular requirements,

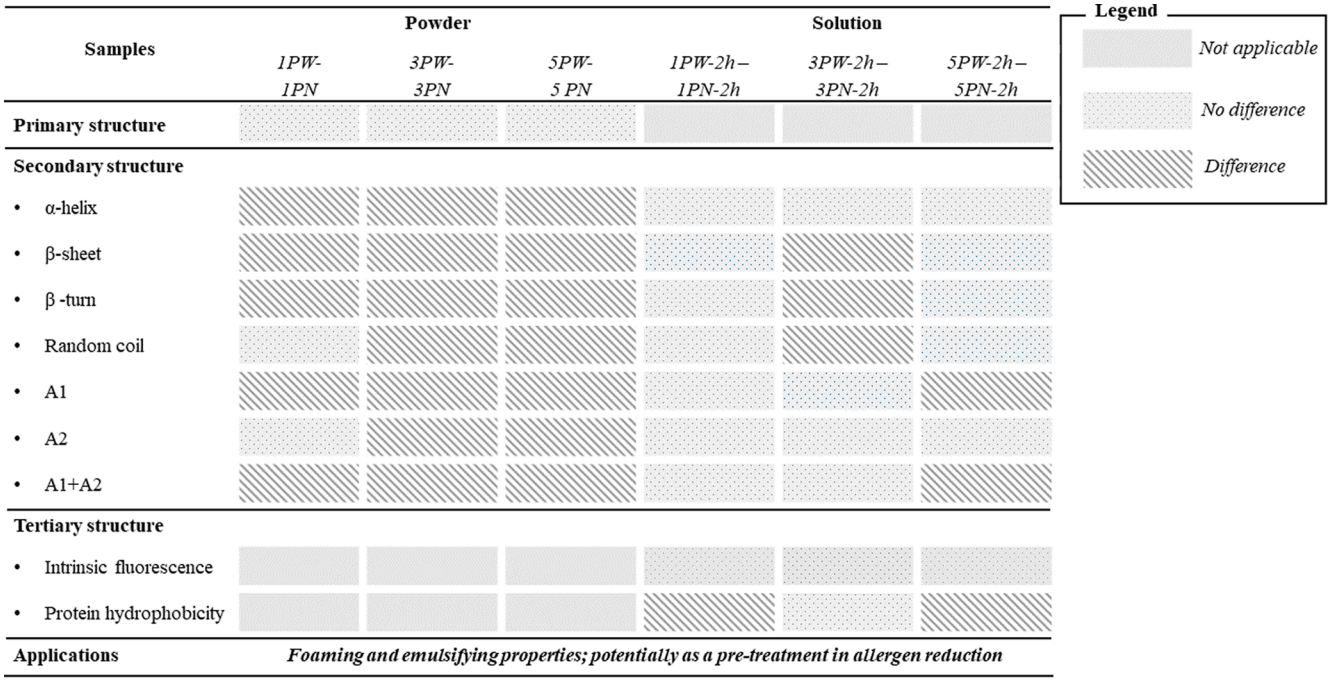

Fig. 8. Summary of the effect of microfluidization on the soybean protein structures and potential applications.

microfluidization can serve as a method to enhance foaming and emulsifying characteristics and potentially serve as a preliminary treatment for reducing allergens.

4. Conclusions

This paper studied the impact of high shear force, cavitation, and high pressure produced by microfluidization on the primary, secondary, and tertiary structures of soybean protein isolate by comparing different conditions, including the temperature and number of passes. Regarding the primary structure, the SDS-PAGE analysis under reducing conditions showed that the protein bands remained unchanged when exposed to microfluidization treatment. On the other hand, microfluidization treatment impacted the secondary structure of the protein in a solid state, and these differences remained after re-solubilization in water, as measured by FTIR. The high shear force can influence the protein digestibility and flexibility for the solid state, leading to protein unfolding. Moreover, at a higher number of passes (>3), the resulting mechanical forces seem to cause protein rearrangement and aggregation. Furthermore, no differences were observed for secondary structural features at 3 and 5 passes for both studied thermal conditions (temperature controlled or not). More interestingly, it is for the secondary structure of the proteins in the solution, where the structure changes completely when the powders are reconstituted in water, with a significant difference only in α-helix, β-sheet and β-turn. Lyophilization could explain this difference in results compared with the solid state because this process also subjects protein and peptide molecules to unique stressors, causing potential modifications in conformation. Moreover, microfluidization could also contribute to this effect by decreasing the particle size and opening more sites, therefore encouraging ice crystal formation before freeze drying. Regarding the tertiary structure, an impact of microfluidization on soybean protein isolate was observed. Microfluidization increases the surface hydrophobicity, and some hydrophobic amino acid residues become exposed due to the intense effect of high shear forces, high pressure, and cavitation. This could improve the functional properties of proteins, such as foaming or emulsifying. However, the most significant difference was observed for 5PW.

CRediT authorship contribution statement

Andreea Diana Kerezsi: Writing – review & editing, Writing – original draft, Visualization, Methodology, Investigation, Formal analysis, Data curation, Conceptualization. **Nicolas Jacquet:** Writing – review & editing, Visualization, Validation, Supervision, Methodology, Funding acquisition, Conceptualization. **Oana Lelia Pop:** Writing – review & editing, Writing – original draft, Validation, Conceptualization. **Ines Othmeni:** Visualization, Methodology, Formal analysis, Data curation. **Antoine Figula:** Writing – original draft, Methodology, Formal analysis, Data curation. **Frédéric Francis:** Visualization, Validation, Methodology, Formal analysis. **Gaoussou Karamoko:** Methodology, Formal analysis, Data curation. **Romdhane Karoui:** Visualization, Supervision, Methodology, Formal analysis, Data curation. **Christophe Blecker:** Writing – review & editing, Visualization, Validation, Supervision, Methodology, Investigation, Funding acquisition.

Declaration of competing interest

The authors declare that they have no known competing financial interests or personal relationships that could have appeared to influence the work reported in this paper.

Data availability

Data will be made available on request.

Acknowledgments

The authors gratefully acknowledge Walloon Region for supporting this work as part of the ALLERSOJA project (WIN2WAL program, convention 1910044). Also, the authors would like to thank Andrew Zicler (Teaching and Research Center, Gembloux, Belgium) for providing the shape Z chamber of the microfluidizer and Chakraborty Arpita (Teaching and Research Center, Gembloux, Belgium) for the support regarding the statistical analysis. We are grateful to Kelly Light (McGill University, Sainte-Anne-de-Bellevue, Canada) for supporting the statistical analysis and improving the article's English level. Also, the authors gratefully acknowledge Emilie Bera (Functional & Evolutionary Entomology, Gembloux Agro-BioTech, Belgium) for teaching the technique SDS-PAGE.

References

Abbott, T. P., Nabetani, H., Sessa, D. J., Wolf, W. J., Liebman, M. N., & Dukor, R. K. (1996). Effects of Bound Water on FTIR Spectra of Glycinin. *Journal of Agricultural and Food Chemistry, 44*(8), 2220–2224. https://doi.org/10.1021/JF950340H

Arakawa, T., Prestrelski, S. J., Kenney, W. C., & Carpenter, J. F. (2001). Factors affecting short-term and long-term stabilities of proteins. *Advanced Drug Delivery Reviews, 46* (1–3), 307–326. https://doi.org/10.1016/S0169-409X(00)00144-7

Aschemann-Witzel, J., Gantriis, R. F., Fraga, P., & Perez-Cueto, F. J. A. (2021). Plant-based food and protein trend from a business perspective: Markets, consumers, and the challenges and opportunities in the future. *Critical Reviews in Food Science and Nutrition, 1–10*. https://doi.org/10.1080/10408398.2020.1793730

Blancher, C., & Jones, A. (2001). SDS -PAGE and Western Blotting Techniques. *Methods in Molecular Medicine, 57*, 145–162. https://doi.org/10.1385/1-59259-136-1:145

Bouaouina, H., Desrumaux, A., Loisel, C., & Legrand, J. (2006). Functional properties of whey proteins as affected by dynamic high-pressure treatment. *International Dairy Journal, 16*(4), 275–284. https://doi.org/10.1016/J.IDAIRYJ.2005.05.004

Boubellouta, T., & Dufour, É. (2012). Cheese-Matrix Characteristics During Heating and Cheese Melting Temperature Prediction by Synchronous Fluorescence and Mid-infrared Spectroscopies. *Food and Bioprocess Technology, 5*(1), 273–284. https://doi.org/10.1007/S11947-010-0337-1

Carbonaro, M., Maselli, P., & Nucara, A. (2012). Relationship between digestibility and secondary structure of raw and thermally treated legume proteins: A Fourier transform infrared (FT-IR) spectroscopic study. *Amino Acids, 43*(2), 911–921. https://doi.org/10.1007/S00726-011-1151-4

Carbonaro, M., & Nucara, A. (2010). Secondary structure of food proteins by Fourier transform spectroscopy in the mid-infrared region. *Amino Acids, 38*(3), 679–690. https://doi.org/10.1007/S00726-009-0274-3/FIGURES/4

Carpenter, J. F., Arakawa, T., & Crowe, J. H. (1992). Interactions of stabilizing additives with proteins during freeze-thawing and freeze-drying. *Developments in Biological Standardization*.

Carpenter, J. F., & Crowe, J. H. (1989). An infrared spectroscopic study of the interactions of carbohydrates with dried proteins. *Biochemistry, 28*(9), 3916–3922. https://doi.org/10.1021/BI00435A044

Carpenter, J. F., Pikal, M. J., Chang, B. S., & Randolph, T. W. (1997). Rational design of stable lyophilized protein formulations: Some practical advice. *Pharmaceutical Research, 14*(8), 969–975. https://doi.org/10.1023/A:1012180707283

Chen, H., Hong, Q., Zhong, J., Zhou, L., Liu, W., Luo, S., & Liu, C. (2019). The enhancement of gastrointestinal digestibility of β-LG by dynamic high-pressure microfluidization to reduce its antigenicity. *International Journal of Food Science & Technology, 54*(5), 1677–1683. https://doi.org/10.1111/IJFS.14044

Chen, Y., Tu, Z., Wang, H., Zhang, L., Sha, X., Pang, J., Yang, P., Liu, G., & Yang, W. (2016). Glycation of β-lactoglobulin under dynamic high pressure microfluidization treatment: Effects on IgE-binding capacity and conformation. *Food Research International, 89*, 882–888. https://doi.org/10.1016/J.FOODRES.2016.10.020

Chok, K. C., Ng, M. G., Ng, K. Y., Koh, R. Y., Tiong, Y. L., & Chye, S. M. (2021). Edible Bird's Nest: Recent Updates and Industry Insights Based On Laboratory Findings. *Frontiers in Pharmacology, 12*, Article 746656. https://doi.org/10.3389/FPHAR.2021.746656

Codex Alimentarius. (2022). *GENERAL STANDARD FOR SOY PROTEIN PRODUCTS, CXS 175-1989* (Issue 8.5.2017).

De Boer, J., & Aiking, H. (2011). On the merits of plant-based proteins for global food security: Marrying macro and micro perspectives. *Ecological Economics, 70*(7), 1259–1265. https://doi.org/10.1016/J.ECOLECON.2011.03.001

Dissanayake, M., & Vasiljevic, T. (2009). Functional properties of whey proteins affected by heat treatment and hydrodynamic high-pressure shearing. *Journal of Dairy Science, 92*(4), 1387–1397. https://doi.org/10.3168/JDS.2008-1791

Djemaoune, Y., Cases, E., & Saurel, R. (2019). The Effect of High-Pressure Microfluidization Treatment on the Foaming Properties of Pea Albumin Aggregates. *Journal of Food Science, 84*(8), 2242–2249. https://doi.org/10.1111/1750-3841.14734

Dong, X., Wang, J., & Raghavan, V. (2020). Critical reviews and recent advances of novel non-thermal processing techniques on the modification of food allergens. *Critical Reviews in Food Science and Nutrition, 61*(2), 196–210. https://doi.org/10.1080/10408398.2020.1722942

Etzion, Y., Linker, R., Cogan, U., & Shmulevich, I. (2004). Determination of Protein Concentration in Raw Milk by Mid-Infrared Fourier Transform Infrared/Attenuated Total Reflectance Spectroscopy. *Journal of Dairy Science, 87*(9), 2779–2788. https://doi.org/10.3168/JDS.S0022-0302(04)73405-0

Fang, L., Xiang, H., Sun-Waterhouse, D., Cui, C., & Lin, J. (2020). Enhancing the Usability of Pea Protein Isolate in Food Applications through Modifying Its Structural and Sensory Properties via Deamidation by Glutaminase. *Journal of Agricultural and Food Chemistry, 68*(6), 1691–1697. https://doi.org/10.1021/ACS.JAFC.9B06046

Gong, K., Chen, L., Xia, H., Dai, H., Li, X., Sun, L., Kong, W., & Liu, K. (2019). Driving forces of disaggregation and reaggregation of peanut protein isolates in aqueous dispersion induced by high-pressure microfluidization. *International Journal of Biological Macromolecules, 130*, 915–921. https://doi.org/10.1016/J.IJBIOMAC.2019.02.123

Guo, X., Chen, M., Li, Y., Dai, T., Shuai, X., Chen, J., & Liu, C. (2020). Modification of food macromolecules using dynamic high pressure microfluidization: A review. *Trends in Food Science & Technology, 100*, 223–234. https://doi.org/10.1016/J.TIFS.2020.04.004

He, X., Chen, J., He, X., Feng, Z., Li, C., Liu, W., Dai, T., & Liu, C. (2021). Industry-scale microfluidization as a potential technique to improve solubility and modify structure of pea protein. *Innovative Food Science & Emerging Technologies, 67*, Article 102582. https://doi.org/10.1016/J.IFSET.2020.102582

Hu, C. Q., Chen, H. B., Gao, J. Y., Luo, C. P., Ma, X. J., & Tong, P. (2011). High-pressure microfluidisation-induced changes in the antigenicity and conformation of allergen Ara h2 purified from Chinese peanut. *Journal of the Science of Food and Agriculture, 91*(7), 1304–1309. https://doi.org/10.1002/JSFA.4318

Hu, J., Yu, B., Yuan, C., Tao, H., Wu, Z., Dong, D., Lu, Y., Zhang, Z., Cao, Y., Zhao, H., Cheng, Y., & Cui, B. (2023). Influence of heat treatment before and/or after high-pressure homogenization on the structure and emulsification properties of soybean protein isolate. *International Journal of Biological Macromolecules, 253*, Article 127411. https://doi.org/10.1016/J.IJBIOMAC.2023.127411

Islam, F., Amer Ali, Y., Imran, A., Afzaal, M., Zahra, S. M., Fatima, M., Saeed, F., Usman, I., Shehzadi, U., Mehta, S., & Shah, M. A. (2023). Vegetable proteins as encapsulating agents: Recent updates and future perspectives. *Food Science & Nutrition, 11*(4), 1705–1717. https://doi.org/10.1002/FSN3.3234

Jideani, V. A. (2011). Functional Properties of Soybean Food Ingredients in Food Systems. In *Soybean - Biochemistry, Chemistry and Physiology*. InTech. https://doi.org/10.5772/14668.

Kerezsi, A. D., Jacquet, N., & Blecker, C. (2022). Advances on physical treatments for soy allergens reduction - A review. *Trends in Food Science & Technology, 122*, 24–39. https://doi.org/10.1016/J.TIFS.2022.02.007

L'Hocine, L., & Boye, J. I. (2007). Allergenicity of soybean: new developments in identification of allergenic proteins, cross-reactivities and hypoallergenization technologies. *Critical reviews in food science and nutrition, 47*(2), 127–143. https://doi.org/10.1080/10408390600626487

Laemmli, U. K. (1970). Cleavage of structural proteins during the assembly of the head of bacteriophage T4. *Nature, 227*(5259), 680–685. https://doi.org/10.1038/227680a0

Lee, H., Yildiz, G., dos Santos, L. C., Jiang, S., Andrade, J. E., Engeseth, N. J., & Feng, H. (2016). Soy protein nano-aggregates with improved functional properties prepared by sequential pH treatment and ultrasonication. *Food Hydrocolloids, 55*, 200–209. https://doi.org/10.1016/J.FOODHYD.2015.11.022

Li, T., Bu, G., & Xi, G. (2021). Effects of heat treatment on the antigenicity, antigen epitopes, and structural properties of β-conglycinin. *Food Chemistry, 346*, Article 128962. https://doi.org/10.1016/J.FOODCHEM.2020.128962

Li, Y., Deng, L., Dai, T., Li, Y., Chen, J., Liu, W., & Liu, C. (2022). Microfluidization: A promising food processing technology and its challenges in industrial application. *Food Control, 137*, Article 108794. https://doi.org/10.1016/J.FOODCONT.2021.108794

Liao, Y. H., Brown, M. B., Quader, A., & Martin, G. P. (2002). Protective mechanism of stabilizing excipients against dehydration in the freeze-drying of proteins. *Pharmaceutical Research, 19*(12), 1854–1861. https://doi.org/10.1023/A:1021497625645/METRICS

Ling, B., Ouyang, S., & Wang, S. (2019). Effect of radio frequency treatment on functional, structural and thermal behaviors of protein isolates in rice bran. *Food Chemistry, 289*, 537–544. https://doi.org/10.1016/J.FOODCHEM.2019.03.072

Liu, C. M., Zhong, J. Z., Liu, W., Tu, Z. C., Wan, J., Cai, X. F., & Song, X. Y. (2011). Relationship between Functional Properties and Aggregation Changes of Whey Protein Induced by High Pressure Microfluidization. *Journal of Food Science, 76*(4), E341–E347. https://doi.org/10.1111/J.1750-3841.2011.02134.X

Long, G., Ji, Y., Pan, H., Sun, Z., Li, Y., & Qin, G. (2015). Characterization of Thermal Denaturation Structure and Morphology of Soy Glycinin by FTIR and SEM. *International Journal of Food Properties*. https://doi.org/10.1080/10942912.2014.908206, 18(4), 763-774. 10(1080/10942912), pp. 908206, 2014

Luo, L., Wang, Z., Deng, Y., Wei, Z., Zhang, Y., Tang, X., Liu, G., Zhou, P., Zhao, Z., Zhang, M., & Li, P. (2022). High-pressure homogenization: A potential technique for transforming insoluble pea protein isolates into soluble aggregates. *Food Chemistry, 397*. https://doi.org/10.1016/J.FOODCHEM.2022.133684

Martínez, K. D., Ganesan, V., Pilosof, A. M. R., & Harte, F. M. (2011). Effect of dynamic high-pressure treatment on the interfacial and foaming properties of soy protein isolate–hydroxypropylmethylcelluloses systems. *Food Hydrocolloids, 25*(6), 1640–1645. https://doi.org/10.1016/J.FOODHYD.2011.02.013

Melchior, S., Moretton, M., Calligaris, S., Manzocco, L., & Nicoli, M. C. (2022). High pressure homogenization shapes the techno-functionalities and digestibility of pea proteins. *Food and Bioproducts Processing, 131*, 77–85. https://doi.org/10.1016/J.FBP.2021.10.011

Nahimana, P., Kerezsi, A. D., Karamoko, G., Abdelmoumen, H., Blecker, C., & Karoui, R. (2023). Impact of defatting methods on the physicochemical and functional properties of white lupin protein isolates. *European Food Research and Technology, 1*, 1–14. https://doi.org/10.1007/S00217-023-04305-X

Ozturk, O. K., & Turasan, H. (2021). Latest developments in the applications of microfluidization to modify the structure of macromolecules leading to improved physicochemical and functional properties. *Critical Reviews in Food Science and Nutrition*. https://doi.org/10.1080/10408398.2021.1875981, 62(16), 4481-4503. 10(1080/10408398), pp. 1875981, 2021

Pace, C. N. (1990). Conformational stability of globular proteins. *Trends in Biochemical Sciences, 15*(1), 14–17. https://doi.org/10.1016/0968-0004(90)90124-T

Pan, J., Zhang, Z., Mintah, B. K., Xu, H., Dabbour, M., Cheng, Y., Dai, C., He, R., & Ma, H. (2022). Effects of nonthermal physical processing technologies on functional, structural properties and digestibility of food protein: A review. *Journal of Food Process Engineering, 45*(4), e14010. https://doi.org/10.1111/JFPE.14010

Pelton, J. T., & McLean, L. R. (2000). Spectroscopic Methods for Analysis of Protein Secondary Structure. *Analytical Biochemistry, 277*(2), 167–176. https://doi.org/10.1006/ABIO.1999.4320

Pi, X., Sun, Y., Fu, G., Wu, Z., & Cheng, J. (2021). Effect of processing on soybean allergens and their allergenicity. *Trends in Food Science & Technology, 118*, 316–327. https://doi.org/10.1016/J.TIFS.2021.10.006

Qin, P., Wang, T., & Luo, Y. (2022). A review on plant-based proteins from soybean: Health benefits and soy product development. *Journal of Agriculture and Food Research, 7*, Article 100265. https://doi.org/10.1016/J.JAFR.2021.100265

Rahaman, T., Vasiljevic, T., & Ramchandran, L. (2016). Effect of processing on conformational changes of food proteins related to allergenicity. *Trends in Food Science and Technology, 49*, 24–34. https://doi.org/10.1016/j.tifs.2016.01.001

Rodrigues, I. M., Coelho, J. F. J., & Carvalho, M. G. V. S. (2012). Isolation and valorisation of vegetable proteins from oilseed plants: Methods, limitations and potential. *Journal of Food Engineering, 109*(3), 337–346. https://doi.org/10.1016/J.JFOODENG.2011.10.027

Santo, R. E., Kim, B. F., Goldman, S. E., Dutkiewicz, J., Biehl, E. M. B., Bloem, M. W., Neff, R. A., & Nachman, K. E. (2020). Considering Plant-Based Meat Substitutes and Cell-Based Meats: A Public Health and Food Systems Perspective. *Frontiers in Sustainable Food Systems, 4*, Article 569383. https://doi.org/10.3389/FSUFS.2020.00134

Serrano, S., Rincón, F., & García-Olmo, J. (2013). Cereal protein analysis via Dumas method: Standardization of a micro-method using the EuroVector Elemental Analyser. *Journal of Cereal Science, 58*(1), 31–36. https://doi.org/10.1016/j.jcs.2013.04.006

Shen, L., & Tang, C. H. (2012). Microfluidization as a potential technique to modify surface properties of soy protein isolate. *Food Research International, 48*(1), 108–118. https://doi.org/10.1016/J.FOODRES.2012.03.006

Sui, X., Zhang, T., & Jiang, L. (2021). Soy protein: Molecular structure revisited and recent advances in processing technologies. *Annual Review of Food Science and Technology, 12*, 119–147. https://doi.org/10.1146/annurev-food-062220-104405

Tang, C. H. (2017). Emulsifying properties of soy proteins: A critical review with emphasis on the role of conformational flexibility. *Critical Reviews in Food Science and Nutrition, 57*(12), 2636–2679. https://doi.org/10.1080/10408398.2015.1067594

Thakral, S., Sonje, J., Munjal, B., & Suryanarayanan, R. (2021). Stabilizers and their interaction with formulation components in frozen and freeze-dried protein formulations. *Advanced Drug Delivery Reviews, 173*, 1–19. https://doi.org/10.1016/J.ADDR.2021.03.003

Türker-Kaya, S., & Huck, C. W. (2017). A review of mid-infrared and near-infrared imaging: principles, concepts and applications in plant tissue analysis. *Molecules, 22*(1), 168. https://doi.org/10.3390/MOLECULES22010168

Turoverov, K. K., & Kuznetsova, I. M. (2003). Intrinsic Fluorescence of Actin. *Journal of Fluorescence, 13*(1), 41–57. https://doi.org/10.1023/A:1022366816812

Vera, A., Valenzuela, M. A., Yazdani-Pedram, M., Tapia, C., & Abugoch, L. (2019). Conformational and physicochemical properties of quinoa proteins affected by different conditions of high-intensity ultrasound treatments. *Ultrasonics Sonochemistry, 51*, 186–196. https://doi.org/10.1016/J.ULTSONCH.2018.10.026

Wang, C., Wang, J., Zhu, D., Hu, S., Kang, Z., & Ma, H. (2020). Effect of dynamic ultra-high pressure homogenization on the structure and functional properties of whey protein. *Journal of Food Science and Technology, 57*(4), 1301–1309. https://doi.org/10.1007/S13197-019-04164-Z

Wang, J., He, Z., & Raghavan, V. (2023). Soybean allergy: characteristics, mechanisms, detection and its reduction through novel food processing techniques. *Critical Reviews in Food Science and Nutrition, 63*(23), 6182–6195. https://doi.org/10.1080/10408398.2022.2029345

Wang, Z., Li, Y., Jiang, L., Qi, B., & Zhou, L. (2014). Relationship between secondary structure and surface hydrophobicity of soybean protein isolate subjected to heat treatment. *Journal of Chemistry, 2014*. https://doi.org/10.1155/2014/475389

Wu, F., Shi, X., Zou, H., Zhang, T., Dong, X., Zhu, R., & Yu, C. (2019). Effects of high-pressure homogenization on physicochemical, rheological and emulsifying properties of myofibrillar protein. *Journal of Food Engineering, 263*, 272–279. https://doi.org/10.1016/J.JFOODENG.2019.07.009

Yan, S., Xu, J., Zhang, S., & Li, Y. (2021). Effects of flexibility and surface hydrophobicity on emulsifying properties: Ultrasound-treated soybean protein isolate. *LWT, 142*, Article 110881. https://doi.org/10.1016/J.LWT.2021.110881

Zheng, L., He, M., Zhang, X., Regenstein, J. M., Wang, Z., Ma, Z., Kong, Y., Wu, C., Teng, F., & Li, Y. (2021). Gel properties and structural characteristics of soy protein isolate treated with different salt ions before spray drying combined with dynamic high-pressure micro-fluidization. *Food and Bioproducts Processing, 125*, 68–78. https://doi.org/10.1016/J.FBP.2020.10.016

Zheng, T., Li, X., Taha, A., Wei, Y., Hu, T., Fatamorgana, P. B., Zhang, Z., Liu, F., Xu, X., Pan, S., & Hu, H. (2019). Effect of high intensity ultrasound on the structure and physicochemical properties of soy protein isolates produced by different

denaturation methods. *Food Hydrocolloids, 97*, Article 105216. https://doi.org/10.1016/j.foodhyd.2019.105216

Zhong, J., Luo, S., Liu, C., & Liu, W. (2014). Steady-state kinetics of tryptic hydrolysis of β-lactoglobulin after dynamic high-pressure microfluidization treatment in relation to antigenicity. *European Food Research and Technology, 239*(3), 525–531. https://doi.org/10.1007/S00217-014-2248-2

Zhu, Y., Fu, S., Wu, C., Qi, B., Teng, F., Wang, Z., Li, Y., & Jiang, L. (2020). The investigation of protein flexibility of various soybean cultivars in relation to physicochemical and conformational properties. *Food Hydrocolloids, 103*, Article 105709. https://doi.org/10.1016/J.FOODHYD.2020.105709